Available online at www.sciencedirect.com
ScienceDirect
Ceramics International 33 (2007) 1217–1222
CERAMICS INTERNATIONAL
www.elsevier.com/locate/ceramint

Si/SiC ceramics from wood of Indian dicotyledonous mango tree

D. Mallick [a], O.P. Chakrabarti [a,*], H.S. Maiti [a], R. Majumdar [b]

[a] *Central Glass and Ceramic Research Institute, Kolkata-700032, India*
[b] *Department of Chemical Technology, University of Calcutta, Kolkata-700009, India*

Received 29 July 2005; received in revised form 9 February 2006; accepted 31 March 2006
Available online 6 September 2006

Abstract

Synthesis of cellular Si/SiC ceramics using native dicotyledonous plants was investigated. Mango (*Mangifera indica*) represents a typical dicotyledonous plant. Wood of mango tree having typical structural features was transformed by controlled pyrolysis into carbonaceous preforms and subsequently converted into Si/SiC ceramics by liquid Si-infiltration at ~1600 °C under vacuum. The pyrolyzed mango was characterized in terms of pyrolysis weight loss, shrinkages, bulk density and microstructures. The resulting ceramics have maximum density of 2.66 g/cm^3 with porosity of 0.5 vol.% and contain silicon carbide (SiC), residual Si, in addition to pores or carbon (trace). The conversion process preserves the microcellular morphology of the parent wood tissue anatomy in the ceramic structure. Typically, Si/SiC-mango has room temperature flexural strength of 247 MPa, Young's modulus of 253 GPa, hardness of 1182 kg/mm^2 and shows small gain in weight of ~2% during oxidative heating up to 1300 °C in flowing air.

Keywords: C. Mechanical property; Dicotyledonous mango wood; Si/SiC ceramics; Cellular morphology

1. Introduction

Synthesis of engineering ceramics and composites in the image of biostructures has received much attention in recent years [1–5]. The morphological and structural variations in materials of plant origin – such as wood, stem, roots, leaf, fruit, flower, seed and seed cover (e.g. rice husk), grass, fibers (e.g. jute, hemp) and so on offer unique opportunity in designing and synthesizing the materials of innumerably different shapes and microstructures that are, at the present state of knowledge and practice, either prohibitively costly or unthinkable to be synthesized through the conventional routes of powder, melt, slurry or solution processing.

Transformation of bioorganic structures, especially plant structures inherent in wood and stem into cellular duplex Si/SiC ceramic composites have been dealt with in a number of recent publications and patents [6–15]. The most common practice is to make use of some wood or wood like material, suitably pieced and/or shaped, in the preparation of a carbonized preform under controlled condition of thermal processing and allow the latter to react with silicon bearing liquid or gas under vacuum or in an inert atmosphere.

Synthesis of SiC based ceramics and Si/SiC composite ceramic biomimetically from caudex stem of a few monocotyledonous plants of Indian origin and preliminary characterization of them have been reported earlier [16,17]. A recent communication deals with the preliminary aspects of the processing and characterization of cellular Si/SiC ceramics derived by replicating the structure of some Indian dicotyledonous woods [18]. The present article deals further with processing and characterization of Si/SiC ceramic from Indian dicotyledonous mango wood and attempts at a comparison by thermal analysis of dicot mango wood and monocot coconut stem as plant precursors for synthesis of Si/SiC based engineering ceramics. Stabilities of Si/SiC ceramics derived from dicot wood (mango) and monocot stem (coconut) were also compared by thermogravimetry under oxidizing conditions up to ≥1200 °C.

2. Experimental

2.1. Pyrolytic conversion of plant material into carbonaceous preform

Wood of a common dicotyledonous plant of local origin (mango (*Mangifera indica*)) was used as the precursor, the

* Corresponding author. Tel.: +91 33 2473 3496; fax: +91 33 2473 0957.
E-mail address: omprakash@cgcri.res.in (O.P. Chakrabarti).

0272-8842/$32.00
doi:10.1016/j.ceramint.2006.03.028

Table 1
Characteristics of native dicotyledonous mango wood

Molecular composition (wt%)					Density (g cm^{-3})	Drying loss (wt%)	Drying shrinkage (%)		
α-Cellulose[a]	Hemicellulose[a]	Lignin[a]	Ash[b]	Moisture[b,c]			Axial	Radial	Tangential
37.60	26.64	31.80	1.29	11.68	0.57	9.93	0.13	1.96	3.36

[a] Based on the weight of oven dry defatted wood.
[b] Based on the weight of oven dry wood.
[c] At 65% R.H.

characteristic of which is given in Table 1. Wood specimen was shaped, dried and pyrolyzed by heating up to 800 °C under self-generated atmosphere in an electrically heated furnace to yield rectangular biocarbon preform (70 mm × 13 mm × 13 mm), following the procedure described elsewhere [14]. It was further characterized in terms of pyrolytic weight loss, shrinkage, bulk density and microstructure; the conversion of wood into biocarbon preform was also examined using simultaneous thermal analysis (STA) technique.

2.2. Synthesis and characterization of cellular Si/SiC ceramic

The biocarbon preform from mango wood was infiltrated and reacted with molten silicon (purity 99.41 wt%; Indian Metals and Ferro Alloys, India) under vacuum at a temperature of around 1600 °C for 40 min in a graphite resistance heated furnace (Astro, Thermal Technologies, Santa Barbara, CA) to yield duplex Si/SiC ceramic. The final material was characterized for density by water displacement method and porosity by boiling water method, phase identification by X-ray diffraction (XRD) analysis (PW1710, Philips, Holland); microstructural examination was done using scanning electron microscopy (SEM) (SE-440, Leo-Cambridge, Cambridge, UK) and thermal analysis (TGA) using a thermo-balance (STA 490C, Netzcsh-Geratebau GmbH, Germany) up to 1300 °C in flowing air at a rate of 10 K/min. For a comparison, Si/SiC ceramic composite derived from stem of a monocotyledonous plant, coconut [16] was also subjected to TG up to 1200 °C in flowing air at a rate of 10 K/min. Three-point bending strength and Young's modulus of Si/SiC ceramic material (specimens of 45 mm × 3.5 mm × 2.5 mm, ground and polished up to 1 μm finish) were determined at room temperature using an Instron Universal Testing Machine and the deflection was monitored through a LVDT with a resolution of 0.05% of full scale deflection. Five tests were conducted and an average value has been reported. Hardness was measured at 50 g load in a microhardness tester (Ernst Leitz Vicker Hardness Tester, Leitz GmbH, Wetzlar, Germany) with residence period of 12 s. A standard Vicker's diamond pyramid indenter was used for measuring hardness (H) using the relation: $H = 1.854P/(2a)^2$ kg/mm^2, where P is the indentation load in kg and $2a$ is the average length of the indentation diagonal in mm. Twenty indentations were made at the indentation load and average value was reported.

3. Results and discussions

3.1. Pyrolytic conversion of plant materials into carbonaceous preforms

3.1.1. Pyrolytic weight loss and shrinkage

Thermal analysis of native mango wood was performed in flowing nitrogen at a heating rate of 10 K/min. The TG curve (Fig. 1(a)) has four segments—an abrupt low loss up to ∼120 °C, followed by a high loss starting at ∼250–280 °C and ending at ∼380–400 °C, a reduced weight loss up to ∼600 °C, and finally a very nominal and continued weight loss up to 1240 °C. While the first step weight loss may be attributed to removal of physically absorbed water, the second major step of weight loss is due likely to decomposition of hemicellulose, cellulose and lignin which exhibit maxima at 280, 340 and 400 °C in their respective decomposition [7]. The accompanying DTA curve (Fig. 1(b)) for native mango wood specimen shows weak exothermic peak at ∼300 °C followed by a relatively strong exothermic peak at ∼600 °C. These peaks may, presumably, be attributed to oxidative decomposition involving the biopolymeric oxygen and breakdown of the –C–C– chains of the polynuclear carbon structures of hemicellulose, cellulose and lignin. The slow weight loss beyond 600 °C (Fig. 1(a)) probably involves peripheral oxidation of skeletal carbon formed aided by oxygenated molecules formed in situ. The third exothermic DTA peak at ∼1070 °C (Fig. 1(b)), may be indicative of structural ordering of amorphous carbon. To compare the responses during thermal analysis for dicotyledonous woods and monocotyledonous stems of Indian origin, TG and DTA of monocot stem of coconut was separately performed under identical conditions of thermal analysis as of dicot mango wood. The TG and DTA scans exhibit features that are similar to those for mango wood but there are also significant deviations. For example, there are shifts in the temperatures of steps of weight loss and the last exothermic peak for coconut stem is strong and predominant and takes place at a temperature above 1100 °C. The molecular composition of coconut stem was separately determined following the procedure as has been applied for mango; the content of α-cellulose, hemicellulose and lignin, ash and moisture were found to be 41.1%, 22.9%, 32.9%, 1.5% and 11.2%, respectively. The differences in responses during thermal analysis for the two types of plant precursors may be attributed to changes in molecular compositions and to structural and microstructural variations in them.

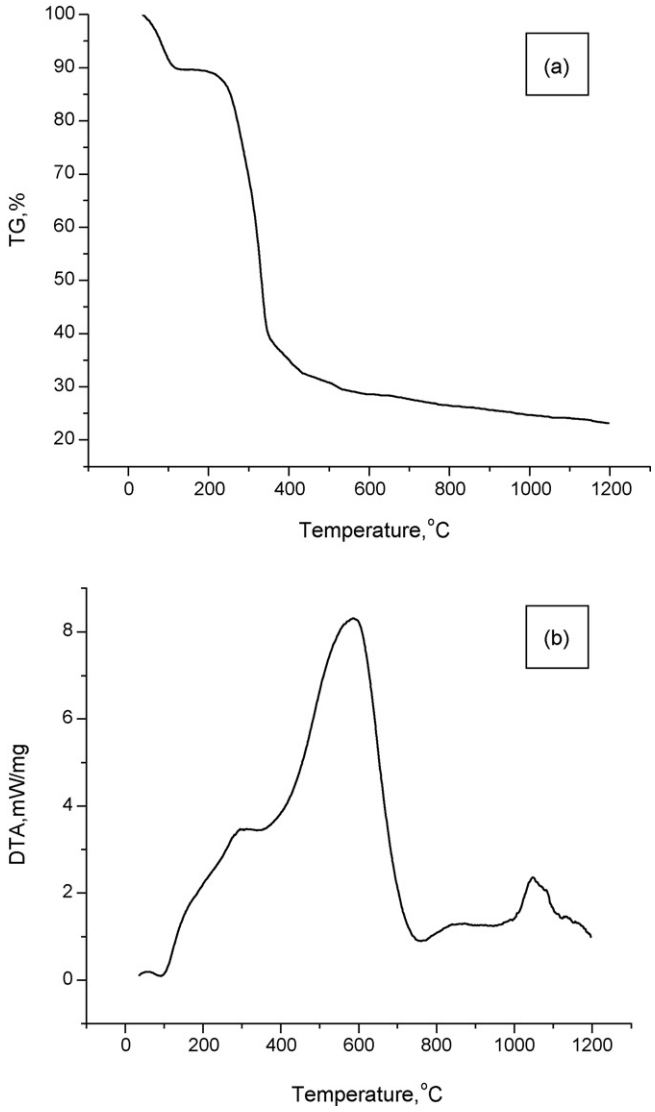

Fig. 1. (a) Weight loss during heating of native mango wood in flowing N_2 atmosphere (heating rate 10 K/min); (b) DTA curve for native mango wood specimens in flowing N_2 atmosphere (heating rate 10 K/min; reference = Al_2O_3).

During separate pyrolysis run the mango wood specimens exhibit average weight losses of around 69% of dry mass, lower by about 10% than the corresponding TG weight loss. This is because of the drying loss of the native undried wood samples used in the TG runs. It has pyrolytic shrinkages of ~22%, 30–33% and 26–28% in axial, tangential and radial direction, respectively. The density of pyrolyzed mango varies from 0.39 to 0.47 g cm^{-3}. Under identical conditions of pyrolysis, coconut stem exhibits a weight loss of 71% and shrinkages of 22%, 31% and 32% along the length (axis), width and thickness, respectively [16].

3.1.2. Microstructure of biocarbon

Fig. 2(a and b) gives the respective microstructural views of tangential–radial (TR) and axial–radial (AR) sections of biocarbon preform from mango wood, showing characteristic arrangement of carbon web along with interconnected void structure. Microstructural features are seen to be highly anisotropic and change in different directions with respect to the growth axis of the native plant. Diameters of pores originating from vascular vessels and tracheidal channels are measured from the micrographs and found to be 95–105 and 2–20 μm, respectively. Monocot stems also show preservation of structural integrity and microscopic structural features of native plants after pyrolysis, despite a vast change in linear dimension [16].

3.2. Synthesis of cellular Si/SiC ceramics

3.2.1. Density, porosity and dimensional change

Spontaneous infiltration of the biocarbon preforms derived from mango wood took place when the porous biopreform was brought into contact with silicon melt under vacuum. All the specimens got fully infiltrated and reacted throughout into dense structures with complete retention of the macroscopic structural integrity in 40 min. In case of Si/SiC ceramics made from mango the shrinkages vary within 0.2–0.7%, 0.1–1.6% and 0.2–0.8% in the axial, radial and tangential directions, respectively. Si-infiltrated pyrolyzed mango exhibits fluctuation in the density and porosity within 2.52–2.66 g/cm^3 and 0.5–4.8 vol.%, respectively, which may be attributed to the local changes of the carbon density in the pyrolyzed wood specimens.

Assuming (i) complete infiltration of Si melt into the systemic pores of the carbonaceous preforms and stoichiometric reaction between C and Si, (ii) no dimensional change and (iii) no loss of materials during ceramization, the material properties can be determined by the following empirical

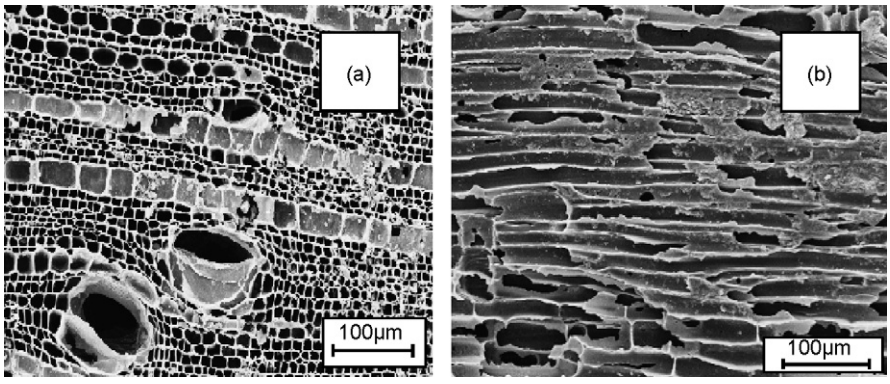

Fig. 2. SEM/SE images (a) tangential–radial (TR) and (b) axial–radial (AR) sections of pyrolyzed mango.

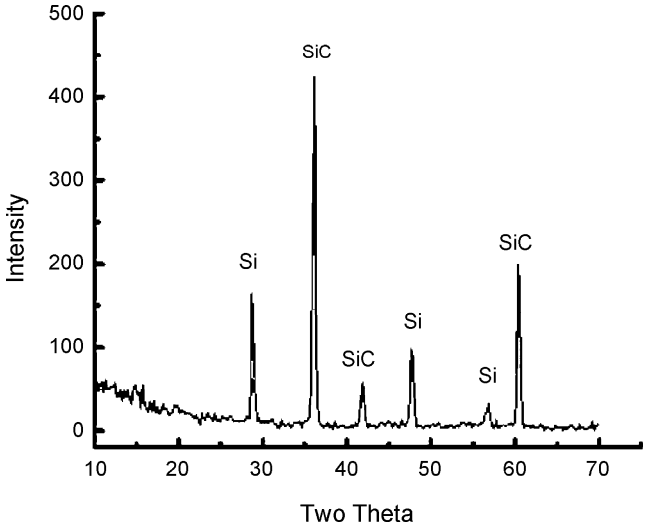

Fig. 3. XRD profile of Si-infiltrated carbonaceous preform from mango showing the presence of Si and β-SiC.

equation. For ideally dense duplex Si/SiC ceramic composites, the ceramic density can be given as:

$$d_{\text{Ceram}} = V_{\text{SiC}} d_{\text{SiC}} + V_{\text{Si}} d_{\text{Si}} = d_{\text{Si}} + 1.038\, d_{\text{CB}} (d_{\text{SiC}} - d_{\text{Si}}) \quad (1)$$

where V_{SiC} and V_{Si} are the fractional volumes of SiC and Si present in the duplex Si/SiC ceramic composites and $V_{\text{SiC}} = (d_{\text{CB}} M_{\text{SiC}})/(d_{\text{SiC}} M_{\text{C}}) = 1.038 d_{\text{CB}}$, d_{CB} and M_{C} being the density of carbon preform and molecular weight of carbon (12 g/mol), d_{SiC} and M_{SiC} the density and molecular weight of SiC (40 g/mol), respectively and d_{Si} the density of Si. For an average carbon density of 0.43 g/cm^3 (as measured for mango carbon), Eq. (1) gives a ceramic density of 2.72 g/cm^3. Based on this value and the density fluctuation obtained in the present study, fluctuation in the relative density can be computed to be varying within 92.7–98.2%, predicting variation of porosity in the range of 1.8–7.3%. The variation of porosity obtained in the present study (0.5–4.8 vol.%), thus, closely tallies with the predicted range of porosity. Incidentally, pyrolyzed coconut has a density of 0.45 g/cm^3 and Si-infiltrated pyrolyzed coconut has the density and porosity of 2.72 g/cm^3 and 0.7 vol.%, respectively [16]. Ceramic density of 2.74 g/cm^3 can be predicted by Eq. (1) for carbon density of 0.45 g/cm^3. Thus, a relative density of 99.27% can be computed predicting a porosity value of 0.73% which tallies very closely with the experimentally obtained value of 0.7 vol.%.

3.2.2. XRD analysis

The XRD-scan from a Si infiltrated pyrolyzed mango wood is shown in Fig. 3. β-SiC and Si are the only crystalline phases present.

3.2.3. Microstructure

SEM/BSE images of the Si melt infiltrated pyrolyzed mango sample show that the microstructural features of the initial native preform are well preserved during transformation into ceramic structures (Fig. 4). The appearance of dense microstructure is common in both the tangential–radial (TR) (Fig. 4(a)) and the axial–radial (AR) sections (Fig. 4(b)). Three phases are observed: (i) predominant dark grey regions, (ii) light grey zones and (iii) occasional deep black spots (regions (i) and (ii) mostly appear together). Phases (i) and (ii) are identified as SiC and Si, respectively, by EDX analysis and the deep black spots are identified as pores and/or residual carbon. Preservation of microstructural features of preforms during transformation of pyrolyzed coconut stems into ceramic structures has also been noticed [16].

The pyrolyzed mango originally showed tracheidal porous channels with diameter in the range of 2–20 μm and such pores are seen to be nearly completely filled with solidified Si after processing. The carbon of the pyrolyzed preform converts to β-SiC and the residual Si fills the pore interiors. In the tangential–radial section of infiltrated specimens large vascular channel pores with diameters ranging between 95 and 105 μm, that remain unfilled with Si, are seen.

The presence of Si-filled and unfilled porosity in infiltrated specimens from pyrolyzed dicotyledonous mango wood may be explained by the theory of capillary infiltration. The maximum pore diameter (d_{max}) for spontaneous infiltration into a capillary perpendicular to the melt surface, is given as [19]:

$$d_{\text{max}} = \frac{4\gamma \cos\theta}{\rho g h} \quad (2)$$

where h is the infiltration depth, θ the wetting angle, γ and ρ the surface tension and density of the infiltrating melt and g the acceleration due to gravity. However, there are very few data at present on the properties of Si melt. We can use surface tension

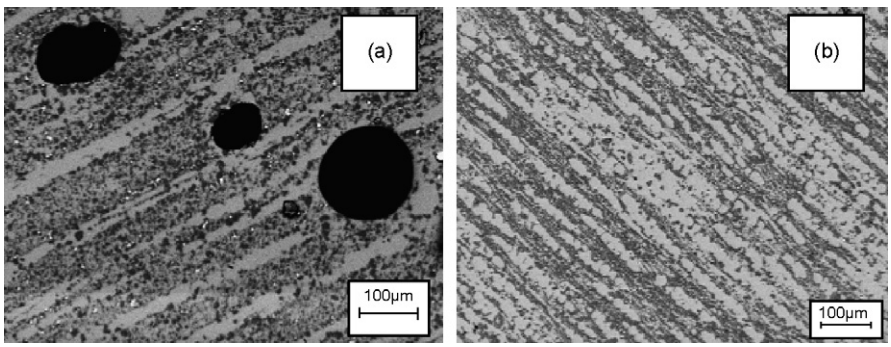

Fig. 4. Preservation of cellular structural features in ceramics derived from dicot mango wood as is evident in its SEM/BSE images of (a) TR- and (b) AR-sections.

$\gamma = 0.75$ N m^{-1} based on data for vacuum at 1550 °C [20] and $\theta = 40°$ for liquid Si on carbon [21]. Considering that the density of the Si melt at the infiltration temperature will be equal to its density at the melting point (1420 °C), i.e., 2.55 g cm^{-3} [20] and taking an infiltration depth (h) of 1 m as a reasonable order of magnitude [20], a d_{max} of 92 μm is derived from Eq. (2). This corresponds well with the experimental results which showed that in case of biocarbon preform from dicotyledonous mango wood, large pores (with diameters greater than ~90 μm) originating from the vascular channels, remain unfilled, while tracheidal pores (with diameters smaller than ~90 μm) in the preforms are nearly completely filled with solidified Si. It may be noted that in case of Si/SiC composite derived from stem of a monocot plant, viz. coconut, all the pores are less than ~90 μm and are all filled with Si [16].

3.2.4. Oxidation resistance

Thermogravimetry of the Si/SiC ceramics from mango (Fig. 5) exhibited a small increase in weight of 1.57% during heating to 1300 °C in flowing air, indicating sufficient resistance of the final ceramic in high temperature oxidative environment. The increase in weight is probably due to the formation of protective SiO_2 surface layer as a product of oxidation. This SiO_2 is expected to have prevented further ingress of oxygen to react with SiC and Si [22]. TG of Si/SiC composite derived from coconut stem also shows considerable resistance to oxidation up to 1200 °C [17].

3.2.5. Flexural strength and Young's modulus

The room temperature three-point flexural strength and Young's modulus were evaluated to be 241 ± 27 MPa and 253 ± 22 GPa, respectively, for Si/SiC-mango of density 2.59 g/cm^3 and porosity 2.65 vol.%. Conventional reaction bonded SiC (RBSC) ceramics, also containing SiC and Si-phases and having density of 3.06 g/cm^3 and porosity of 1.73 vol.%, exhibits strength and modulus values of 254 ± 25 MPa and 316 ± 23 GPa, respectively [23]. The Si/SiC ceramic from mango has lower density than the conventional RBSC, but has strength and elastic modulus comparable to those of its conventional counterpart. Si/SiC ceramics from coconut also have strength (263 ± 21 MPa) and Young's modulus (247 ± 19 GPa) values [17] comparable to those of Si/SiC-mango and of conventional RBSC.

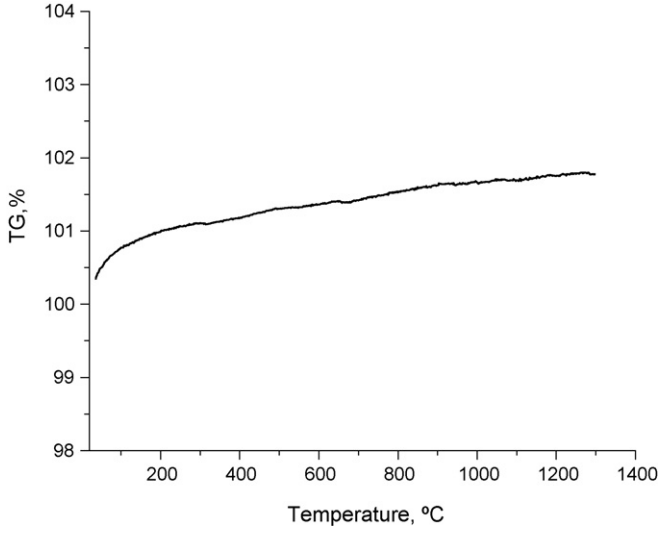

Fig. 5. TGA scan of Si/SiC ceramics made from mango wood during heating up to 1300 °C showing slow and low weight gain.

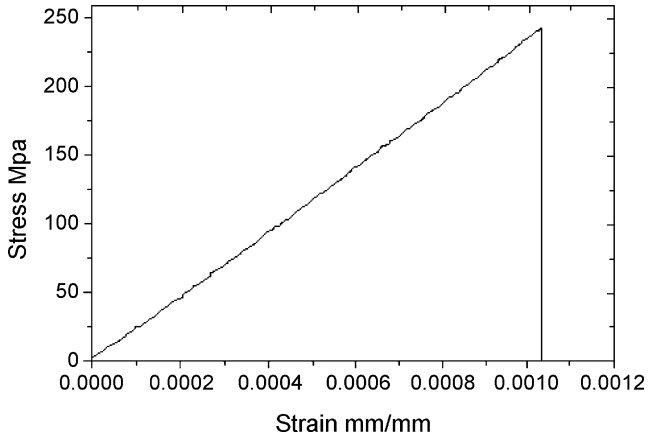

Fig. 6. Typical stress–strain diagram of Si/SiC ceramics derived from mango.

Typical stress–strain diagram of biomorphic Si/SiC ceramics derived from mango is shown in Fig. 6. The specimen was loaded in a direction perpendicular to the tracheidal pore system. It behaved in linear elastic fashion until catastrophic failure occurred at strain-to-failure of around 0.11%. The representative micrograph of the fracture surface is shown in Fig. 7. It shows the distribution of cylindrical pores (originating from vascular vessels) with a significant amount of alignment. It also reveals that cleavage dominates the process of fracture.

3.2.6. Hardness

The hardness of the Si-infiltrated pyrolyzed mango was obtained as 1181.97 ± 97.39 kg/mm^2 at 50 g load. Both Si and SiC grains present in the composite, interact with the indenter and are responsible for the resulting hardness of the final material. On the basis of its average density and porosity values, the volume fraction of Si and SiC may be computed as 60.78%

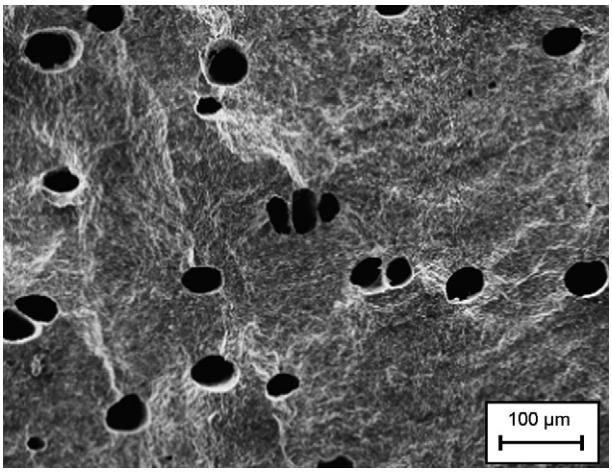

Fig. 7. SEM/SE image of fracture surface of Si/SiC ceramics from mango.

and 36.57%, respectively. Assuming uniform distribution of Si- and SiC-phases with respective hardness of 1000 and 2600 kg/mm^2 [24], a resultant hardness of 1558 kg/mm^2 is obtained on the basis that the rule of mixture governs the resultant hardness of a duplex ceramics like Si/SiC [25,26]. The difference between the observed and predicted hardness values as well as the large variance of measured hardness for Si/SiC cellular ceramics from mango, may be attributed to the directional and localized distribution of constituent phases in the end ceramic, evolved in accordance with the anisotropic structure of the parent wood and biocarbon preform.

4. Conclusions

Liquid Silicon Infiltration Processing (LSIP) of pyrolyzed dicot wood from mango of Indian origin, yielded duplex Si/SiC ceramic composites in the image of precursor plant morphology and structure. Depending on the microcellular architecture of the initial plant material, final ceramic composites exhibit a wide variation in microstructures. The Si/SiC-mango shows Si-filled porous channels arising out of the tracheidal elements in range of 2–20 μm in diameter and large channel pores originating from the vascular vessels, with diameters ranging between 95 and 105 μm, that remain unfilled with Si. The ceramics derived from mango wood have flexural strength and Young's modulus values comparable to conventionally prepared Si/SiC ceramics from synthetic preforms. Si-infiltrated pyrolyzed mango and coconut show adequate oxidation resistance during heating to high temperatures (>1200 °C). In such conditions of oxidative heating, Si/SiC-mango shows a weight gain of 1.57% at 1300 °C. Both Si- and SiC-phases contribute to the final hardness of the materials, but due to anisotropic and localized distribution of constituent phases the final hardness could not be fully accounted for in terms of rule of mixtures.

Acknowledgements

The authors wish to thank Mr. S.K. Dalui for measuring the flexural strength and Young's modulus, Mr. M. Ray Chawdhuri for hardness test, Mr. N. Ghosh for XRD analysis, Mr. T.K. Chatterjee for thermal analyses (TG/DTA) and Mrs. S. Ray for SEM studies. They also wish to thank the staff-members of Non-Oxide Ceramic and Composite Division, CGCRI for their cooperation and help. They are also thankful to the services rendered by the staff-members of the Department of Chemical Technology, Calcutta University. Finally they are thankful to the Director, CGCRI, for according permission to publish this work. The authors also wish to thank the Department of Science and Technology (DST), Govt. of India, for sponsoring the work (vide sanction no. SR/S3/ME/20/2003-SERC-Engg., dated 29.10.2004).

References

[1] A.V. Srinivasan, G.K. Haritos, F.L. Hedberg, Biomimetics: advancing man-made materials through guidance of nature, Appl. Mech. Rev. 44 (11) (1991) 463–482.
[2] J.F.V. Vincent, G. Jeronimidis, B.H.V. Topping, A.I. Khan, Biomimetics of flexible composites: towards the development of new materials, Biomimetics 1 (4) (1992) 251–263.
[3] P. Calvert, Biomimetic ceramics and composites, Mater. Res. Soc. Bull. 17 (10) (1992) 37–40.
[4] A.H. Heuer, D.J. Fink, V.J. Laraia, J.L. Arias, P.D. Calvert, K. Kendell, G.L. Messing, J. Blackwill, P.C. Rieke, D.H. Thomson, A.P. Wheeler, A. Veis, A.I. Caplan, Innovative materials processing strategies: a biomimetic approach, Science 255 (1992) 1098.
[5] J.E. Mark, P.D. Calvert, Biomimetic, hybrid and in-situ composites, Mater. Sci. Eng. C.1 (1994) 175–186.
[6] T. Ota, M. Takahashi, T. Hibi, M. Ozawa, S. Suzuki, Y. Hikichi, H. Suzuki, Biomimetic process for producing SiC wood, J. Am. Ceram. Soc. 78 (12) (1995) 3409–3411.
[7] P. Greil, T. Lifka, A. Kaindl, Biomorphic cellular silicon carbide ceramics from wood, J. Eur. Ceram. Soc. 18 (14) (1998) 1961–1973.
[8] M. Singh, Environment conscious ceramics, Ceram. Eng. Sci. Proc. 21 (4) (2000) 39–44.
[9] D.W. Shin, S.S. Park, Y.H. Choa, K. Niihara, Si/SiC composites fabricated by infiltration of a Si melt into charcoal, J. Am. Ceram. Soc. 82 (11) (1999) 3251–3253.
[10] E. Vogli, J. Mukerji, C. Hoffman, R. Kladny, H. Sieber, P. Greil, Conversion of oak to cellular silicon carbide by gas-phase reaction with silicon monoxide, J. Am. Ceram. Soc. 84 (6) (2000) 1236–1240.
[11] E. Vogli, H. Sieber, P. Greil, Biomorphic SiC-ceramic prepared by Si-gas phase infiltration of wood, J. Eur. Ceram. Soc. 22 (14–15) (2002) 2663–2668.
[12] H. Sieber, H. Friedrich, D. Schwarze, A. Kaindl, P. Greil, Ceramic light weight structures from paper derived composites, in: J.P. Singh, N.P. Bansal, K. Niihara (Eds.), Ceramic Transactions, vol. 108, The Am. Ceram. Soc., Ohio, 2000, pp. 571–580.
[13] C.E. Byrne, D.E. Nagle, Cellulose derived composites—a new method for materials processing, Mater. Res. Innovat. 1 (1997) 137–145.
[14] O.P. Chakrabarti, H.S. Maiti, R. Majumdar (Council of Scientific and Industrial Research), Indian Patent, 0481 NF 2002/IN, 22 July, 2004.
[15] O.P. Chakrabarti, H.S. Maiti, R. Majumdar (Council of Scientific and Industrial Research), Indian Patent, 0480 NF/2002/IN, 27 July, 2004.
[16] O.P. Chakrabarti, H.S. Maiti, R. Majumdar, Si/SiC ceramics from plant precursor, J. Mater. Sci. 39 (14) (2004) 4715–4717.
[17] O.P. Chakrabarti, H.S. Maiti, R. Majumdar, Biomimetic synthesis of cellular SiC based ceramics from plant precursor, Bull. Mater. Sci. 27 (5) (2004) 467–470.
[18] O.P. Chakrabarti, D. Mallick, H.S. Maiti, R. Majumdar, Microcellular Si/SiC ceramics by replication of Indian dicotyledonous woods: processing and characterization, Trans. Ind. Ceram. Soc. 65 (1) (2006) 23–28.
[19] F. Daniels, R.A. Alberty, Physical Chemistry, third ed., Wiley, New York, 1967, pp 278–279.
[20] W. Krenkel, F. Gern, Microstructure and characteristics of CMC manufactured via liquid phase route, in: Proceedings of the Ninth International Conference on Composite Materials, ICCM-9, Madrid, Spain, 12–16 July, 1993.
[21] T.J. Whalen, A.T. Anderson, Wetting of SiC, Si_3N_4 and carbon by Si and binary Si alloys, J. Am. Ceram. Soc. 58 (9–10) (1975) 396–399.
[22] O.P. Chakrabarti, J. Mukerji, Oxidation kinetics of reaction sintered silicon carbide, Bull. Mater. Sci. 16 (4) (1993) 325–329.
[23] O.P. Chakrabarti, S. Ghosh, J. Mukerji, Influence of grain size, free Si content and temperature on the strength and toughness of reaction bonded silicon carbide, Ceram. Int. 20 (5) (1994) 283–286.
[24] J.J. Gilman, Hardness—a strength microprobe, in: J.H. Westbrook, H. Conrad (Eds.), The Science of Hardness Testing and Its Research Applications, American Society for Metals, Ohio, USA, 1973, p. 60.
[25] P. Kennedy, Effect of microstructural features on the mechanical properties of REFEL self-bonded silicon carbide, in: S. Hampshire (Ed.), Non-oxide Technical and Engineering Ceramics, Elsevier Applied Science, London, UK, 1986, pp. 301–317.
[26] O.P. Chakrabarti, P.K. Das, J. Mukerji, Influence of free silicon content on the microhardness of RBSiC, Ceram. Forum Int. 74 (2) (1997) 98–101.